Adaptor Protein LAPF Recruits Phosphorylated p53 to Lysosomes and Triggers Lysosomal Destabilization in Apoptosis

Nan Li,[1] Yuanyuan Zheng,[1] Wei Chen,[2] Chunmei Wang,[1] Xingguang Liu,[1] Weigang He,[2] Hongmei Xu,[1] and Xuetao Cao[1,2]

[1]Institute of Immunology and National Key Laboratory of Medical Immunology, Second Military Medical University, Shanghai, P.R. China and [2]Institute of Immunology, Zhejiang University, Hangzhou, Zhejiang, P.R. China

Abstract

Evidence suggests a functional association between the tumor suppressor p53 and apoptosis-involved organelle lysosome; however, the detailed mechanisms remain poorly understood. We recently reported that a lysosome-targeting protein, LAPF (lysosome-associated and apoptosis-inducing protein containing PH and FYVE domains), could initiate apoptosis of L929 cells through a lysosomal-mitochondrial pathway. In this study, we show that LAPF specifically interacted with phosphorylated p53 ($Ser^{15/18}$) both *in vitro* and *in vivo*, which could be enhanced by apoptotic stimuli, such as tumor necrosis factor α (TNF-α) and ionizing irradiation. The PH domain of LAPF and the transactivation domain of p53 mediated the interaction between both molecules. Phosphorylated p53 ($Ser^{15/18}$) could translocate to lysosomes before lysosomal membrane permeabilization (LMP) in LAPF-initiated and TNF-induced apoptosis. Silencing of LAPF expression abrogated lysosomal translocation of phosphorylated p53 ($Ser^{15/18}$), whereas silencing of p53 expression had no effect on lysosomal translocation of LAPF. Similar to that of LAPF silencing, silencing of endogenous p53 expression in L929 cells could significantly impair TNF-α–induced LMP and apoptosis. However, reexpression of wild-type p53, p53S15D (substitution of Ser^{15} to Asp that mimics a phosphorylated state), and p53R175H (a transcription-deficient mutant) in p53-knockdown L929 cells could rescue the decrease in TNF-induced apoptosis. The data suggest that phosphorylated p53 ($Ser^{15/18}$) might translocate to lysosome via forming complexes with adaptor protein LAPF and subsequently result in LMP and apoptosis, which might be in a transcription-independent manner. [Cancer Res 2007;67(23):11176–85]

Introduction

p53 has been regarded as an important transcription factor that exerts its proapoptotic activity by transcriptional activation of a growing list of target genes, including Bax, Bid, Puma, Noxa, p53AIP1, and DR5 (1, 2). However, none of them plays a pivotal role in p53-dependent apoptosis in a manner similar to the $p21^{Waf1}$ gene in p53-mediated cell cycle arrest (3). More and more evidence suggest that p53 also induces apoptosis independent of its transcriptional activity. Several studies showed that p53 could trigger apoptosis in the absence of ongoing transcription and protein synthesis (4, 5). Several transcription-deficient mutants of p53, like p53dl214 (contains amino acids 1–214) and $p53Gln^{22}/Ser^{23}$, have the capability of inducing apoptosis (6, 7). In cell-free extracts, p53 could directly activate caspase-3 with the presence of mitochondria (8). Furthermore, the mechanisms that might account for the transcription-independent proapoptotic activity of p53 had been elucidated recently. Mihara et al. found that mitochondria were the direct targets of p53-induced apoptosis, and p53 protein triggered permeabilization of mitochondrial membrane in a transcription-independent manner by forming complexes with the antiapoptotic Bcl-XL and Bcl-2 protein (9). In human vascular smooth muscle cells, p53 activation transiently upregulated Fas expression in cell surface by transporting from the Golgi complex and subsequently sensitized cells to Fas-mediated apoptosis (10). Therefore, a transcription-dependent pathway and a transcription-independent pathway may coexist in p53-mediated apoptosis. Under normal conditions, these two pathways synergize and lead to cell demise rapidly. Which pathway plays the dominant role may depend on cell type and apoptotic stimulus (11).

Most of organelles, including mitochondria, lysosomes, endoplasmic reticulum, and the Golgi apparatus, participate in the regulation of apoptotic cell death. p53 can launch mitochondrial membrane permeabilization through either increasing the expression of proapoptotic proteins in a transcription-dependent manner or directly targeting mitochondria in a transcription-independent manner. Intriguingly, p53 is also functionally associated with lysosomes and may be located at the upstream of lysosomes in the apoptotic pathway. It had been shown that overexpression of p53 protein in M1 mouse myeloid leukemic cells could trigger lysosomal destabilization and result in apoptosis via a lysosomal-mitochondrial pathway (12). The cytokine IL-6, which could abrogate p53-induced apoptosis, also inhibited p53-triggered lysosomal membrane permeabilization (LMP), suggesting that LMP is important for p53 to perform its apoptotic activity (12–14). Moreover, a lysosomal cathepsin, cathepsin D, is indispensable to p53-dependent apoptosis in lymphoid cells, which has been attributed to increasing p53-regulated protein synthesis (15). SIMPLE, a p53-regulated lysosomal membrane protein, might also participate in p53-dependent apoptosis (16). However, the mechanism of lysosomal destabilization triggered by p53 is far from being understood.

We recently identified the novel protein LAPF (lysosome-associated and apoptosis-inducing protein containing PH and FYVE domains), which is the representative of a new protein family, the Phafins (protein containing both PH and FYVE domains). LAPF could induce caspase-independent apoptosis via translocation to lysosomes and subsequently triggering a lysosomal-mitochondrial pathway (17). In this study, we showed that LAPF, as an adaptor protein, could specifically interact with phosphorylated p53 at Ser^{15}

Note: Supplementary data for this article are available at Cancer Research Online (http://cancerres.aacrjournals.org/).

N. Li, Y. Zheng, and W. Chen contributed equally to this work.

Requests for reprints: Xuetao Cao, Institute of Immunology and National Key Laboratory of Medical Immunology, Second Military Medical University, 800 Xiangyin Road, Shanghai 200433, P.R. China. Phone: 86-21-5562-0605; Fax: 86-21-6538-2502; E-mail: caoxt@public3.sta.net.cn.

doi:10.1158/0008-5472.CAN-07-2333

(corresponding to Ser^{18} in murine p53), which could be enhanced by apoptotic stimuli, such as tumor necrosis factor-α (TNF-α). Furthermore, phosphorylated p53 ($Ser^{15/18}$) could translocate to lysosomes preceding LMP, which could be abrogated by silencing of LAPF expression, and silencing of either p53 or LAPF expression could impair TNF-α–induced lysosomal destabilization and apoptosis, suggesting that adaptor protein LAPF might recruit phosphorylated p53 ($Ser^{15/18}$) to lysosomes to trigger LMP. Reexpression of p53wt, p53S15D (mimicking a phosphorylated state of Ser^{15}), and p53R175H (a transcription-deficient mutant) in p53-knockdown L929 cells could rescue the decrease in TNF-induced apoptosis. These findings provided a clue for potential transcription-independent proapoptotic activity of p53.

Materials and Methods

Plasmid construction. Vectors expressing human LAPF (hLAPF)-GFP and 6His-tagged hLAPF (hLAPF-His) protein were constructed as described previously (17). The entire coding sequence of human p53 (hp53) cDNA was amplified from human dendritic cells, subcloned into pcDNA3.1/myc-His(−)B vector, and confirmed by DNA sequencing. myc-6His-tagged expression mutants of LAPF, including LAPFΔPH (lacking N-terminal PH domain, amino acids 141–297), LAPFΔFY (lacking C-terminal FYVE domain, amino acids 1–140), PH (amino acids 39–133), FYVE (amino acids 147–211), CND (C terminal without domains, amino acids 211–279), and Flag-tagged expression mutants of hp53, including transactivation domain (TAD; amino acids 1–100), DNA-binding domain (DBD; amino acids 101–300), 301 to 393 (amino acids 301–393), 1 to 300 (amino acids 1–300), 101 to 393 (amino acids 101–393), and p53R175H (arg^{175} mutated to his) were generated by PCR mutation reactions and confirmed by DNA sequencing.

Cell culture and cell transfection. MCF-7 (human mammary carcinoma), L929 (mouse fibrosarcoma), and H1299 (human non–small cell lung carcinoma) cells were purchased from American Type Culture Collection and cultured in a 37°C incubator with 5% CO_2 in DMEM with 10% fetal bovine serum. Cell transfection was performed using Lipofectamine 2000 reagent (Invitrogen) in accordance with the manufacturer's instructions. To obtain stable expression cell lines, L929 cells transfected with hLAPF or pcDNA3.1/myc-His(−)B (mock) vector (Invitrogen) were selected by G418 (Calbiochem) as described previously and designated as L929-hLAPF and L929-mock, respectively (17). High expression levels of LAPF in L929-hLAPF cells were confirmed by Western blot (17).

Protein binding assay. The full-length cDNA of LAPF was inserted into pGEX-2T (Amersham Biosciences). The soluble glutathione *S*-transferase (GST) fusion protein GST-hLAPF was expressed in *Escherichia coli* and purified by glutathione Sepharose chromatography as described previously (18, 19). For GST pull-down assay, 100 μg purified GST-hLAPF or GST protein alone was incubated with 60 μL glutathione Sepharose 4B (Pierce) at 4°C for 2 h and then incubated with cell extracts that lysed in ice-cold lysis buffer (Cell Signaling Technology) containing proteinase inhibitors (Sigma) and 0.1% Triton X-100 for another 4 h. For immunoprecipitation, GST-LAPF proteins were preincubated with cell lysate for 4 h. Then phosphorylated p53 (Ser^{15}; 16G8) monoclonal antibody (2 μg/mL, Cell Signaling Technology) and protein G agarose (Pierce) were added, and precipitation was performed 6 h later. The precipitates were subjected to Western blot analysis.

For *in vivo* coprecipitation, cells transfected with indicated plasmids were harvested 48 h after transfection and solublized in lysis buffer supplemented with proteinase inhibitors and 0.1% Triton X-100. Lysates (200 μg total proteins) were incubated with 60 μL Ni-NTA beads (Qiagen) for 8 h (20). Alternatively, the lysates were incubated with phosphorylated p53 (Ser^{15}) monoclonal antibody or anti-Flag M2 monoclonal antibody (Sigma), and the complexes were pulled down by immobilized protein G agarose. All binding assays were performed at 4°C. The precipitants were then separated by 12% SDS-PAGE, transferred onto nitrocellulose membranes, and subjected to Western blot analysis.

Antibody preparation and Western blot. The rabbit polyclonal anti-LAPF antibody was prepared as described previously (17). For Western blot, cells were lysed and protein concentration was determined by bicinchoninic acid protein assay (Pierce). Cell lysates (60 μg) were separated by SDS-PAGE gels and transferred to nitrocellulose membranes. The membranes were probed with the following primary antibodies: anti-p53 monoclonal antibody (DO-1; Santa Cruz), phosphorylated p53 (Ser^{6}, Ser^{9}, Ser^{15}, Ser^{20}, Ser^{33}, Ser^{37}, Ser^{46}) rabbit polyclonal antibody (Cell Signaling Technology), anti-Flag antibody, anti-His (H-3) antibody (Santa Cruz), and anti-actin (C-11) antibody (Santa Cruz). Immunoblots were developed using Supersignal West Femto Maximum Sensitivity substrate (Pierce) after incubation with horseradish peroxidase–conjugated secondary antibodies (Cell Signaling Technology).

Immunofluorescence confocal microscopy. Cells were processed for immunofluorescence as described previously (21). Cells grown on glass coverslips were stained with 200 nmol/L Lyso Tracker Red (Invitrogen) for 15 min at 37°C. After washing with PBS thrice, cells were fixed with 4% polyformaldehyde for 20 min at room temperature and permeabilized with 0.2% Triton X-100 in PBS. Cells were then incubated with appropriate primary antibody and secondary antibodies conjugated with fluorescent dyes and observed under fluorescence confocal microscope (LSM confocal microscope, Carl Zeiss). For the staining of phosphorylated p53 (Ser^{15}), primary phosphorylated p53 (Ser^{15}) antibody and FITC-labeled antimouse secondary antibody (Invitrogen) were used for green fluorescence, whereas biotinylated secondary antimouse antibodies (Cell Signaling Technology) and avidin–Texas Red conjugate (Invitrogen) were used for red fluorescence staining. For the staining of LAPF, anti-LAPF antibody and FITC-labeled antirabbit secondary antibody (Invitrogen) were used.

Apoptosis assay. Cells were treated with hTNF-α (R&D Systems) for indicated time and stained with Annexin V/PI (Invitrogen) and then analyzed by flow cytometry as described previously (17). The percentage of viable and death cells were determined from 10,000 cells per sample.

Lysosomal stability assay. Lyso Tracker Red uptake assay was used to assess permeabilization of lysosomal membrane and performed as described previously (17).

Isolation of cytoplasm and nuclei proteins. The isolation of the cytoplasmic and nuclear protein fractions was performed using NE-PER Nuclear and Cytoplasmic Extraction Reagents (Pierce) according to manufacturer's instructions.

Isolation of lysosomes. The purification of lysosomes from cells in a self-generated gradient of Optiprep (Axis-Shield) was performed according to manufacturer's instructions. Optiprep is based on a density gradient compound, Iodixanol, which has been used for isolation of lysosomes from other organelles (22). The purity of the isolated lysosomes was verified by biochemical analysis and Western blot analysis immediately after the isolation. The results showed that actin (cytoplasm marker) and nuc p65 (nuclear marker) could hardly be detected by Western blot analysis, and the specific activities of cytochrome *c* oxidase (mitochondria marker), glucose-6-phosphatase (ER marker), and catalyse (peroxisome marker) could not be detected by biochemical analysis. The integrity of the isolated lysosomes was verified by the specific activity of β-hexosaminidase (23) and by the detection of LAMP-1 by Western blot analysis.

RNA interference. The small interfering RNA (siRNA) vector of mouse p53 (mp53) was purchased from Imgenex. The plasmid was transfected into L929 cells and selected with 600 to 1,000 ng/mL G418 for 2 to 3 weeks. The inhibition of mp53 expression in L929-mp53i cells was confirmed by Western blot. The LAPF RNA interference cells (L929-LAPFi) and the nonspecific RNA interference control cells (L929-ctrli) were constructed as described previously (17).

Statistical analysis. Statistical analysis (Student's *t* test) was performed using the computer program SPSS version 6.1.

Results

LAPF forms complex with phosphorylated p53 ($Ser^{15/18}$). We recently identified an apoptosis-inducing protein, LAPF, from an undescribed protein family, the Phafins. LAPF can induce apoptosis of L929 cells through translocating to lysosomes and triggering permeabilization of lysosomal membrane (17). Therefore, LAPF

induces apoptosis via a lysosomal-mitochondrial pathway, and LMP might be an initiating event. To examine the mechanisms by which LAPF induces apoptosis, it is instructive to identify the proteins that interact with LAPF. Utilizing coprecipitation for hLAPF-His fusion protein and Western blot analysis, we screened a number of proteins that are related to apoptosis, such as phosphorylated p53 at several sites within N-terminal region, some members of Bcl-2 family, and caspases. We found that phosphorylated p53 at Ser^{15} was detected in the LAPF coprecipitants but not in the control sample. Meanwhile, phosphorylated hp53 at other sites, including at positions 6, 9, 20, 33, 37, and 46, was not detected in LAPF coprecipitants (data not shown).

To show the physical interaction between LAPF and p53 *in vitro*, lysates of human MCF-7 and mouse L929 cells, which contained endogenous wild-type hp53 and mp53, respectively, were incubated with purified GST-hLAPF proteins in GST pull-down assay. The results revealed that LAPF specifically bound to phosphorylated hp53 (Ser^{15}) or phosphorylated mp53 (Ser^{18}, corresponded to Ser^{15} in hp53), but not phosphorylated p53 (Ser^{20}; Fig. 1*A*). Contrariwise, GST-hLAPF was detected in the immunoprecipitants obtained with phosphorylated p53 (Ser^{15}) monoclonal antibody (Fig. 1*A*).

To further confirm the interaction between LAPF and phosphorylated p53 ($Ser^{15/18}$) *in vivo*, hLAPF-His expression vectors were transfected into both MCF-7 and L929 cells. Phosphorylated p53 ($Ser^{15/18}$) and exogenously expressed hLAPF were found in a complex, as detected by both coprecipitation with Ni-NTA beads and immunoprecipitation with anti–phosphorylated p53 (Ser^{15}) antibody (Fig. 1*B*). Furthermore, the colocalization between LAPF and phosphorylated p53 ($Ser^{15/18}$) was confirmed by confocal immunofluorescence analysis in L929 cells when cells underwent apoptotic shrinkage 60 h after transfection with LAPF-GFP (data not shown). Taken together, these data indicated that LAPF formed a complex with phosphorylated p53 ($Ser^{15/18}$) both *in vitro* and *in vivo*.

TNF-α promotes the phosphorylation of p53 ($Ser^{15/18}$) and the interaction of phosphorylated p53 with LAPF. It had been established that overexpression of LAPF not only induced apoptosis of L929 cells but also increased cell sensitivity to TNF-α cytotoxicity (17). We then investigated the effect of TNF-α on the interaction of p53 and LAPF. After TNF stimulation, p53 phosphorylation occurred at 4 h and became significant at 6 to 8 h in L929 cells. Phosphorylation of p38 was also detected after TNF stimulation, almost at the same manner as that of p53 ($Ser^{15/18}$; Fig. 2*A*). Besides, p38 inhibitor (SB203580, 10 μmol/L) treatment could abrogate the phosphorylation of p53 ($Ser^{15/18}$) at a large extent (Fig. 2*A*). Thus, TNF-α could increase the phosphorylation of p53, which might involve the activation of p38. GST pull-down assay was then performed to determine the interaction of p53 and LAPF after TNF stimulation. The results showed the physical interaction of both molecules was significantly increased 12 h after TNF treatment (Fig. 2*B*). The endogenous LAPF interacting with p53 ($Ser^{15/18}$) was also increased 6 to 12 h after TNF treatment (Fig. 2*B*). This interaction was further confirmed by confocal analysis in L929 cells. The merged signal of endogenous LAPF (green) and p53 ($Ser^{15/18}$; red) increased, largely at the cytosol, at 6 h and became significant at 12 h after TNF treatment (Fig. 2*C*). Besides, we also examined whether other apoptotic stimuli, such as ionizing irradiation, affect the interaction of p53 and LAPF. As shown in Fig. 2*D*, the phosphorylation level of p53 at $Ser^{15/18}$, as well as the p53 ($Ser^{15/18}$) interacting with GST-LAPF, increased after 4 h of ionizing irradiation in MCF-7 cells. Therefore, apoptotic stimuli, such as TNF-α and ionizing irradiation, could increase the interaction between p53 ($Ser^{15/18}$) and LAPF.

The interaction of LAPF and phosphorylated p53 ($Ser^{15/18}$) is mediated by PH and TAD domains. To further determine the exact domains involved in the interaction between LAPF and phosphorylated p53 ($Ser^{15/18}$), we constructed a series of deletion mutants of both proteins and tested their binding activity by coprecipitation after expression. Mutants for LAPF, including LAPFΔPH, LAPFΔFY, PH, FYVE, and CND, were tagged with 6His and transfected into MCF-7 cells harboring wild-type hp53, respectively (Fig. 3*A*). The complexes were coprecipitated with Ni-NTA beads from cell extracts and detected with phosphorylated p53 (Ser^{15}) antibody by Western Blot analysis. As shown in Fig. 3*A*,

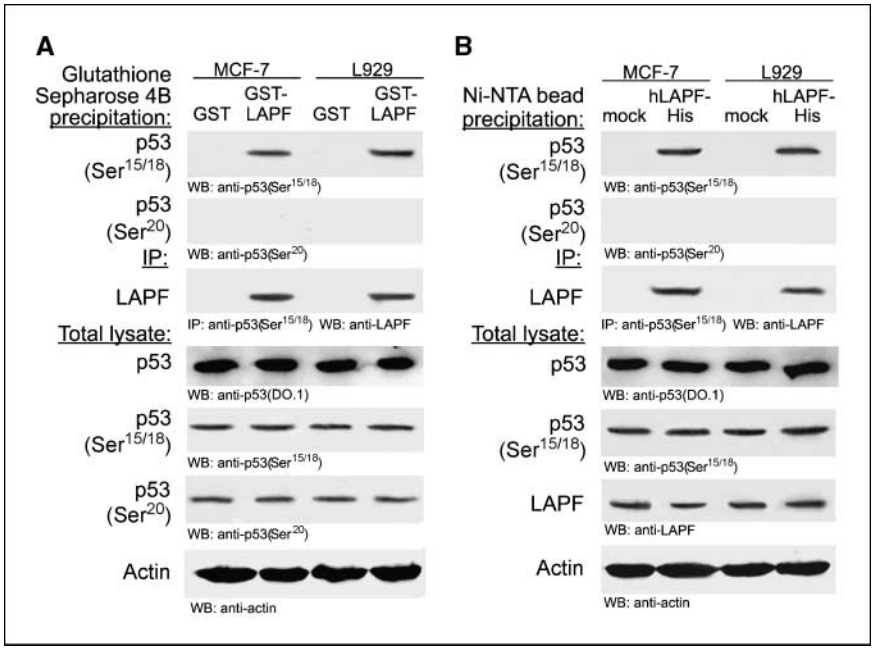

Figure 1. LAPF forms complex with phosphorylated p53 ($Ser^{15/18}$) *in vitro* and *in vivo*. *A,* for GST pull-down assay of *in vitro* binding of LAPF and phosphorylated p53 ($Ser^{15/18}$), an equal amount of GST-hLAPF protein or GST alone was precipitated with glutathione Sepharose 4B beads and then incubated with lysates of MCF-7 or L929 cells. Alternatively, an equal amount of GST-hLAPF protein or GST alone was incubated with lysates of MCF-7 or L929 cells and then immunoprecipitated (*IP*) with anti-p53 ($Ser^{15/18}$) antibody. The precipitants were blotted with the indicated antibodies by Western blot analysis (*WB*). *B,* hLAPF-His or mock vector was transfected into MCF-7 or L929 cells for 60 h. Cell lysates were immobilized with Ni-NTA beads or immunoprecipitated with anti-p53 ($Ser^{15/18}$) antibody. The precipitants were blotted with the indicated antibodies by Western blot analysis.

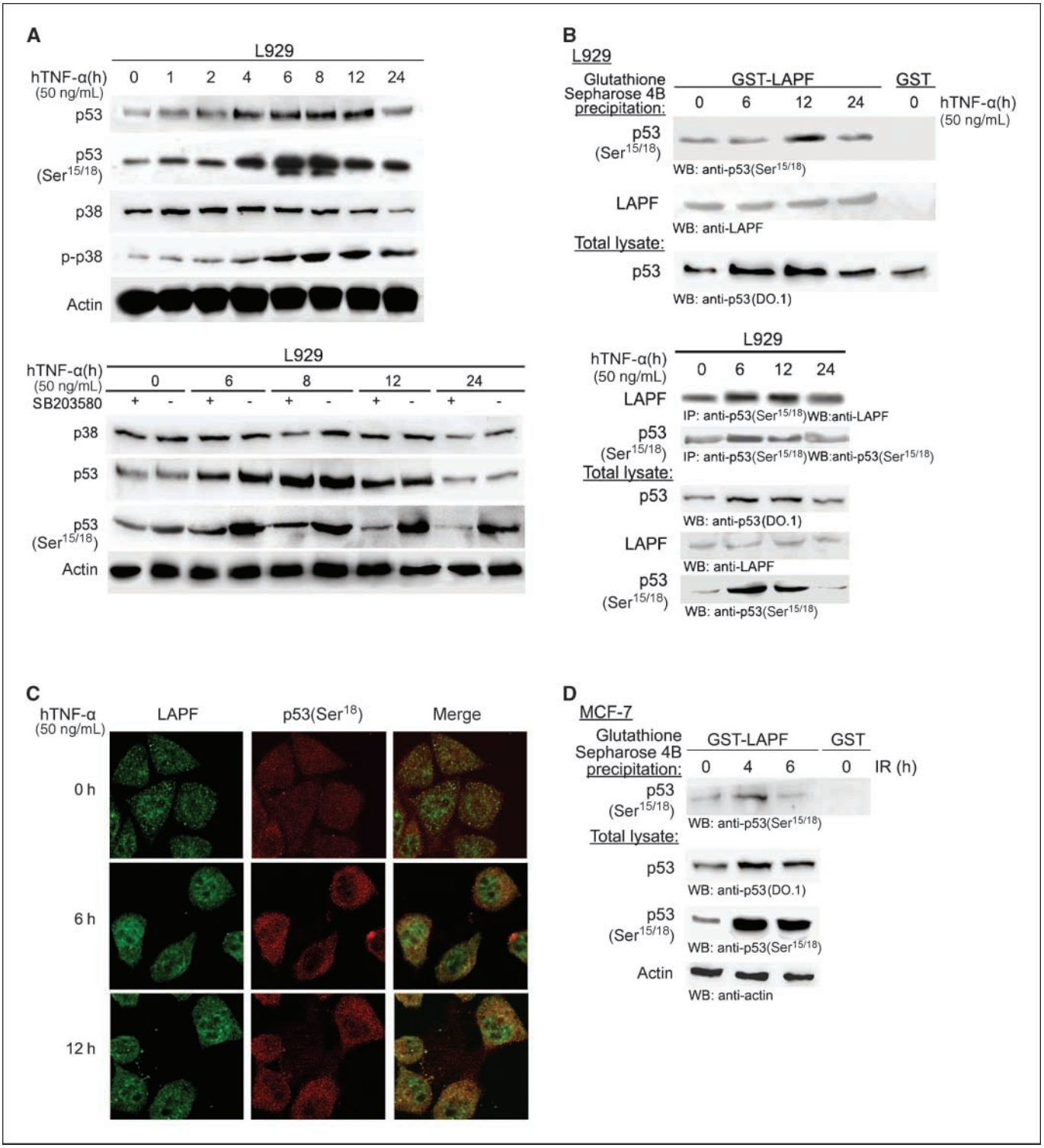

Figure 2. Apoptotic stimuli promote the phosphorylation of p53 ($Ser^{15/18}$) and LAPF-p53 ($Ser^{15/18}$) complex formation. *A,* TNF-α promoted the phosphorylation of p53 ($Ser^{15/18}$) and p38 in L929 cells. L929 cells were treated with hTNF-α (50 ng/mL) for the indicated time and subjected to Western blot analysis with the indicated antibodies. Alternatively, L929 cells were preincubated with the p38 inhibitor SB203580 (10 μmol/L) for 16 h and then stimulated with hTNF-α (50 ng/mL) for the indicated time. Western blot analysis was performed with the indicated antibodies. *B, in vitro* and *in vivo* interaction of LAPF with p53 ($Ser^{15/18}$) in L929 cells after hTNF-α stimulation. For GST pull-down assay, equal amounts of GST fusion proteins were precipitated with glutathione Sepharose 4B beads, incubated with lysates of L929 cells stimulated with TNF-α (50 ng/mL) and immunoblotted with the indicated antibodies. For immunoprecipitation, L929 cells were treated with hTNF-α (50 ng/mL) for the indicated time, and immunoprecipitation was performed by p53 ($Ser^{15/18}$) antibody cross-linked to protein G–agarose. The immunoprecipitants were then subjected to Western blot analysis with the indicated antibodies. *C,* colocalization of phosphorylated p53 (Ser^{18}) with LAPF in L929 cells after hTNF-α stimulation. L929 cells treated with hTNF-α (50 ng/mL) were fixed and stained for LAPF (*green*) with anti-LAPF antibody and phosphorylated p53 (Ser^{18}; *red*) with anti-p53 ($Ser^{15/18}$) antibody and viewed under a confocal microscope. *D,* GST pull-down assay for *in vitro* binding of LAPF with p53 ($Ser^{15/18}$) in MCF-7 cells after ionizing irradiation. Equal amount of GST-hLAPF or GST protein was incubated with lysates of MCF-7 cells after ionizing irradiation (30 Gy), followed by GST pull-down assay. Phosphorylated p53 at $Ser^{15/18}$ was detected by Western blot analysis.

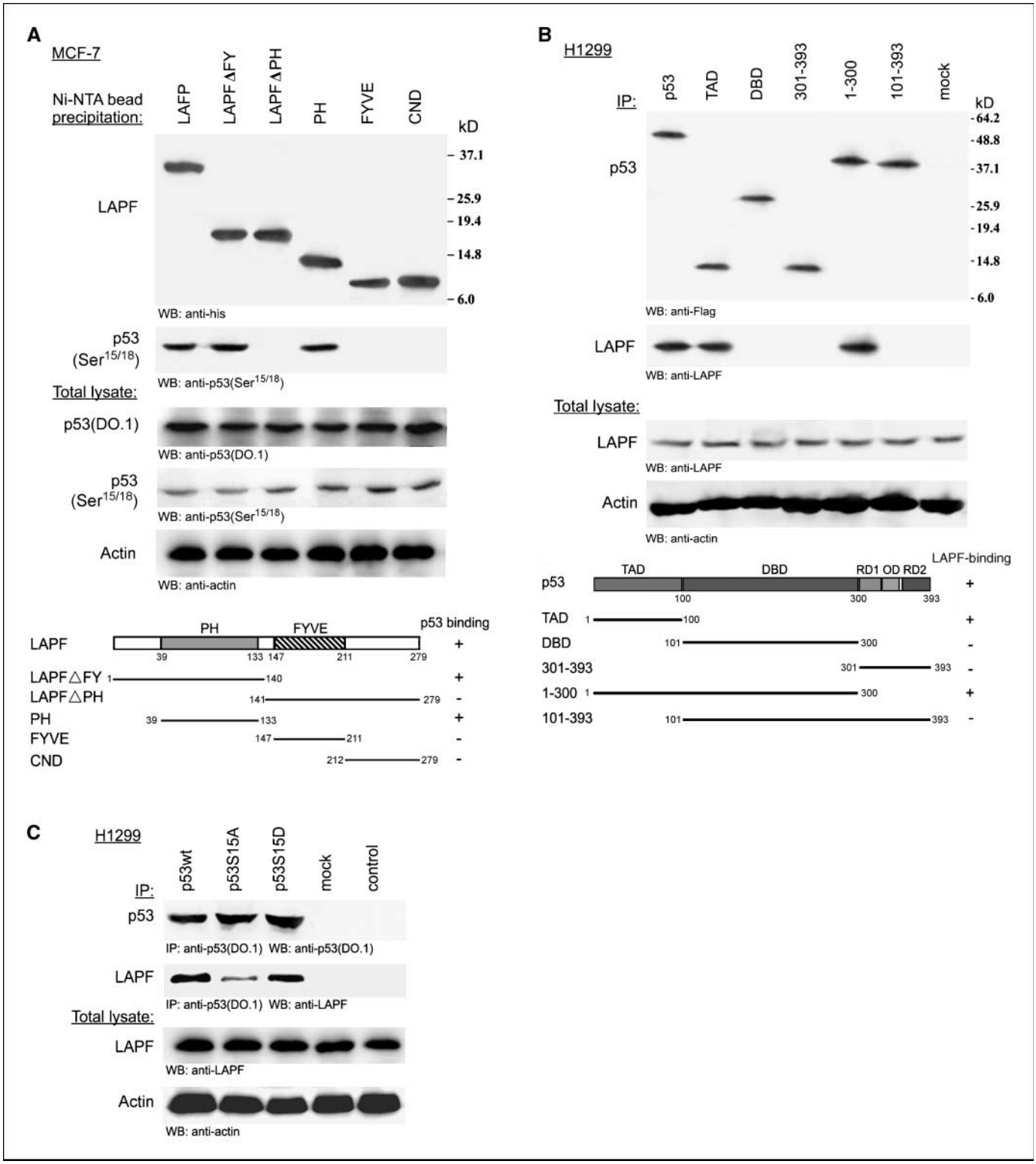

Figure 3. Binding domains for LAPF and phosphorylated p53 (Ser$^{15/18}$). *A,* requirement of N-terminal PH domain of LAPF for binding with phosphorylated p53 (Ser$^{15/18}$). MCF-7 cells were transfected with plasmids encoding deletion mutants of hLAPF-His. 60 h after transfection, cell lysates were immobilized with Ni-NTA-beads. Pellets were washed and subjected to Western blot analysis as indicated. Deletion mutants of hLAPF are schematically drawn, and whether they bind to phosphorylated p53 (Ser$^{15/18}$) or not is indicated with + and -, respectively. The individual domains in LAPF are illustrated: PH: pleckstrin homology domain; FYVE: Fab1, YGLO23, Vps27, and EEA1 domain. The numbers denote the amino acid position. *B,* requirement of N-terminal TAD domain of p53 for binding with LAPF. p53-null H1299 cells were transfected with plasmids encoding deletion mutants of hp53-Flag. At 60 h after transfection, cell lysates were immunoprecipitated with anti-Flag antibody and blotted as indicated. Deletion mutants of hp53 are schematically drawn, and whether they bind to LAPF or not is indicated with + and −, respectively. The individual domains in p53 are illustrated. *OD,* oligomerization domain; *RD,* regulatory domain. The numbers denote the amino acid position. *C,* importance of phosphorylation of Ser^{15} in the p53-LAPF interaction. Lysates from H1299 cells transfected with plasmids encoding mutant of hp53-Flag were immunoprecipitated with anti-p53 (DO.1) antibody and blotted as indicated.

both the PH mutant and LAPFΔFY mutant that contained PH domain were sufficient to bind with phosphorylated p53 (Ser^{15}). In contrast, mutants without PH domain, including LAPFΔPH, FYVE, and CND, failed to interact with phosphorylated p53 (Ser^{15}), although these mutants were expressed at high levels (Fig. 3*A*). These data suggested that LAPF could interact with phosphorylated p53 (Ser^{15}) via its PH domain.

On the other hand, mutants for p53, including TAD, DBD, 301 to 393, 1 to 300, and 101 to 393, were Flag-tagged and cotransfected with LAPF expression vectors into p53-null H1299 cells (Fig. 3*B*). The protein complexes immunoprecipitated with anti-Flag antibody were detected using anti-LAPF antibody. These results indicated that both the single TAD domain and amino acids 1 to 300 interacted with LAPF, whereas mutants without TAD domain (DBD, 301–393, and 101–393) could not form complexes with LAPF. These findings suggested that p53 interacted with LAPF through its TAD domain (Fig. 3*B*).

Because LAPF could specifically bind to p53 phosphorylated at $Ser^{15/18}$, we were interested in whether phosphorylation of Ser^{15} was essential to the interaction between p53 and LAPF. Two site-directed mutants, p53S15A (substitution of Ser^{15} to Ala, a Ser^{15} phosphorylation–negative mutation) and p53S15D (substitution of Ser^{15} to Asp that is a negatively charged amino acid and mimics a phosphorylated state) were used. Notably, the interaction between p53 and LAPF was significantly inhibited when Ser^{15} was substituted to Ala (Fig. 3*C*). Another mutant, p53S15D, interacted with LAPF similar to wild-type p53. Ser^{46} was another important phosphorylation site which might regulate the apoptosis-inducing activity of p53. However, substitution of Ser^{46} to Ala (a nonphosphorylatable amino acid) had no effect on the interaction between p53 and LAPF (data not shown). These data suggested that phosphorylation of Ser^{15} might be important for the p53-LAPF interaction.

Phosphorylated p53 ($Ser^{15/18}$) translocates to lysosomes before permeabilization of lysosomal membrane. We had selected a subclone of L929-hLAPF cells stably expressing LAPF protein at a high level, whereas the expression of LAPF in parental L929 cells was low (17). Several studies reported that 50 ng/mL TNF-α efficiently elicited apoptotic morphologic change of L929 and 10 ng/mL TNF-α failed to trigger apoptosis but significantly reduced cell growth rate (24). As shown in Fig. 4*A* (*left*), exposure to 10 ng/mL hTNF-α resulted in apoptotic cell death of L929-hLAPF cells determined by Annexin V/PI staining, whereas no significant apoptosis was detected in L929 cells transfected with control vectors (L929-mock) and parental L929 cells.

In our previous work, we reported that LAPF facilitated TNF-α–induced apoptosis via initiating permeabilization of lysosomal membrane (17). LMP was detected within 12 h in hTNF-α–treated L929-hLAPF cells, as evidenced by an increased number of "pale cells" (cells with reduced numbers of Lyso Tracker–accumulating lysosomes), and might be an early event to trigger downstream apoptotic pathway (Fig. 4*A, right*). It has been shown that LAPF translocates to lysosomes during apoptosis, and the colocalization of LAPF and lysosomes increases in parallel with the progress of cell demise (17). Because phosphorylated p53 ($Ser^{15/18}$) interacted with LAPF, phosphorylated p53 ($Ser^{15/18}$) might also translocate to cytoplasmic organelles, such as lysosomes. We then isolated the cytoplasmic and nuclear fractions from L929 cells stimulated with hTNF-α. The interaction between p53 ($Ser^{15/18}$) and LAPF could be detected in both fractions. Particularly, in cytoplasmic fraction, the p53 ($Ser^{15/18}$) interacting with endogenous LAPF was increased at 6 h after TNF treatment, whereas in nuclear fraction no change was detected even after 24 h of TNF treatment (Fig. 4*B*). Further analysis by confocal immunofluorescence revealed that the green signal of phosphorylated mp53 (Ser^{18}) began to accumulate to cytosol in L929 cells at 6 h after 50 ng/mL hTNF-α treatment and seemed as a dotted pattern, which coincided partially with the red one of lysosomes (Fig. 4*C*). To confirm the translocation of phosphorylated p53 ($Ser^{15/18}$) to lysosomes, lysosomal fractions of cells stimulated with hTNF-α were isolated using OptiPrep gradient centrifugation. Western blot analysis revealed that the presence of both phosphorylated mp53 (Ser^{18}) and LAPF was first detected in lysosomes isolated from L929-hLAPF cells at 6 h, which was earlier than the occurrence of LMP, and became obvious at 12 h after TNF treatment (Fig. 4*D*). Accordingly, in nonlysosomal cytoplasmic fractions, the decrease of both protein levels in L929-hLAPF cells was significant at 12 h after TNF treatment, which is more rapid than that in L929-mock cells (Supplementary Fig. S1). Therefore, these data indicated that phosphorylated p53 ($Ser^{15/18}$) translocated to lysosomes before LMP during apoptosis.

Silencing of p53 impairs hTNF-α–induced LMP and apoptosis. Despite of the existence of multiple death signaling pathways, a lysosome-mediated pathway had been found to play an important role in a typical apoptotic model, the L929 cells stimulated with 50 ng/mL TNF-α (24). In our experimental system, 50 ng/mL hTNF-α actually induced apoptotic cell death of L929 cells, concomitant with lysosomal membrane destabilization (Fig. 5*A*). Moreover, both LAPF and phosphorylated mp53 (Ser^{18}), which were detected via immunofluorescent staining using anti-LAPF and phosphorylated p53 (Ser^{15}) antibodies, respectively, mainly accumulated to lysosomes 12 h after 50 ng/mL hTNF-α treatment (Fig. 5*B*). We have also shown that apoptosis and LMP induced by 50 ng/mL hTNF-α were significantly inhibited in stable mLAPF-silenced L929 cells (L929-mLAPFi) in which mLAPF was almost undetectable (17). Taken together, it was suggested that LAPF might initiate lysosomal-mitochondrial pathway in this typical apoptotic model and phosphorylated p53 ($Ser^{15/18}$) might be functionally correlated to this apoptotic pathway.

To elucidate the physiologic significance of p53 in apoptosis of L929 cells triggered by 50 ng/mL TNF-α, we examined the functional consequences of RNA interference of endogenous mp53. L929 cells were transfected with vectors containing an mp53-specific RNA interference sequence or a nonspecific control sequence and selected with G418 for stable RNA interference. As shown in Supplementary Fig. S2, the expression of endogenous mp53 proteins were significantly inhibited in stable mp53-silenced cells (L929-mp53i) compared with L929-ctrli cells, and TNF stimulation could hardly affect the mp53 protein levels in L929-mp53i cells. As expected, hTNF-α–initiated apoptosis was markedly inhibited in L929-mp53i cells compared with that in L929-ctrli cells and parental L929 cells (Fig. 5A, *left*). Similarly, hTNF-α–triggered LMP was also significantly attenuated after the expression of mp53 was silenced (Fig. 5A, *right*). These data indicated that p53 might be indispensable to hTNF-α–induced LMP, which in turn resulted in apoptosis.

LAPF may act as an adaptor protein for phosphorylated p53 ($Ser^{15/18}$). It had been shown that both LAPF and phosphorylated p53 ($Ser^{15/18}$) translocated to lysosomes during apoptosis, and silenced expression of these two proteins both led to the inhibition of TNF-α–induced LMP and apoptosis, suggesting that the complex of LAPF and phosphorylated p53 ($Ser^{15/18}$) may be responsible for LMP (17). To explore the exact molecular mechanism for LMP triggering, we used two RNA interference cells, L929-mp53i and

L929-mLAPFi cells, and examined whether silencing of one protein could influence the subcellular localization of the other protein (Supplementary Fig. S2; ref. 17). As shown in Fig. 5*B*, the translocation of phosphorylated mp53 (Ser^{18}) to lysosomes was almost abrogated in L929-mLAPFi cells after hTNF-α stimulation, indicating that LAPF may be essential to the lysosomal localization of phosphorylated p53 ($Ser^{15/18}$). However, LAPF retained the capability of translocating to lysosomes in L929-mp53i cells after hTNF-α exposure (Fig. 5*B*). It could be speculated that phosphorylated p53 ($Ser^{15/18}$) might contribute to hTNF-α–induced LMP, and LAPF might act as an adaptor protein to recruit phosphorylated p53 ($Ser^{15/18}$) to lysosomes.

To confirm the effect of p53 ($Ser^{15/18}$) on TNF-induced LMP and apoptosis, siRNA rescue assay was performed. L929-mp53i cells were transfected with p53wt, p53S15A, or p53S15D mutants. The result revealed that reexpression of p53wt and p53S15D that mimics the phosphorylated state in mp53-knockdown L929 cells could rescue the decrease in TNF-induced apoptosis (Fig. 5*C*).

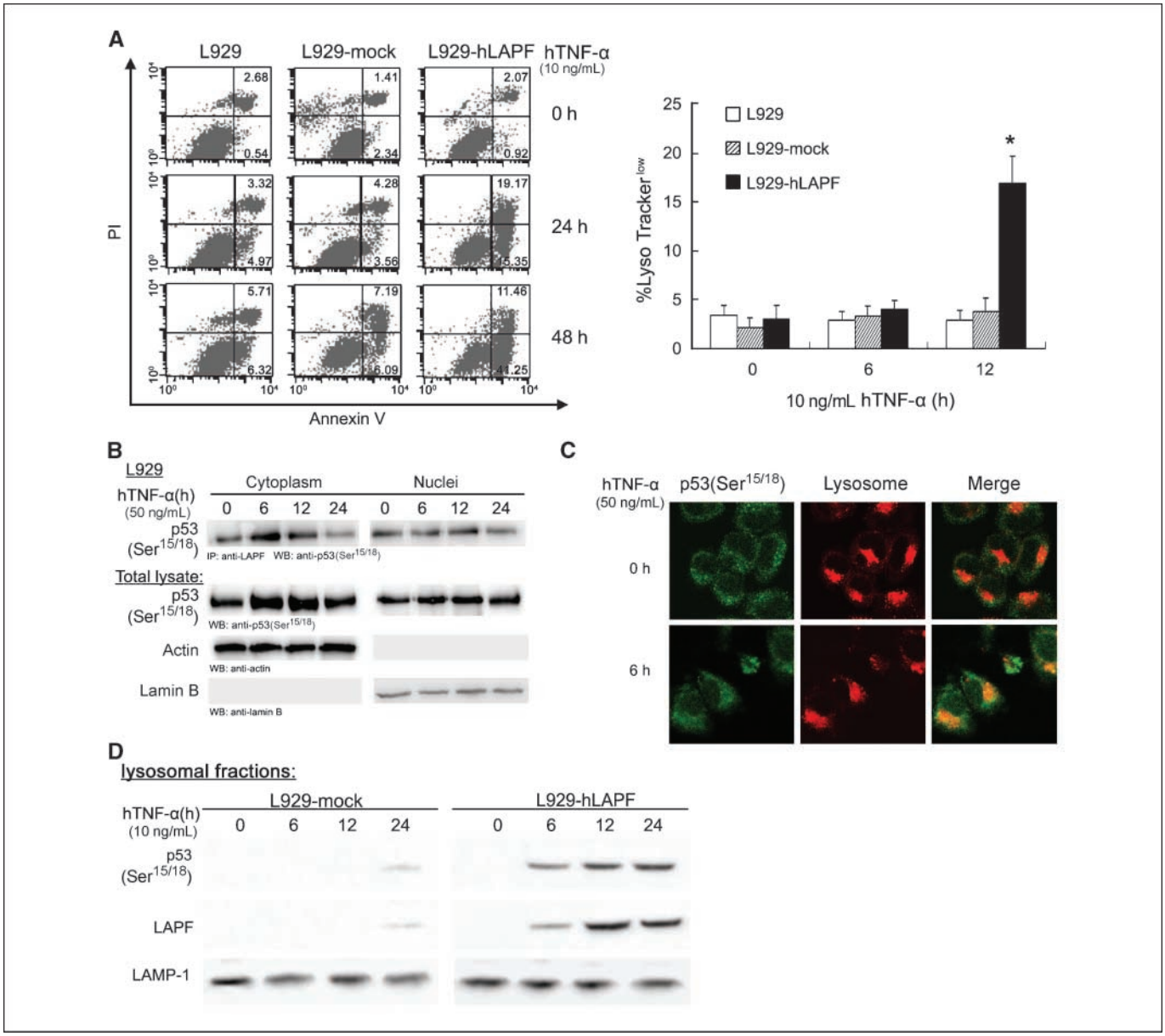

Figure 4. Phosphorylated p53 ($Ser^{15/18}$) translocates to lysosomes before LMP. *A,* sensitivity of L929-hLAPF cells to TNF-α–induced apoptosis and LMP. L929 cells stably expressing hLAPF (L929-hLAPF), L929-mock, or parental L929 cells were treated with 10 ng/mL hTNF-α for the indicated time and stained with Annexin V/PI or Lyso Tracker Red. Apoptosis is represented by the percentage of cells which were Annexin V positive, and results are presented as mean ± SD from three independent experiments. LMP, *columns,* mean percentage of cells exhibiting reduced fluorescence intensity; *bars,* SD. *, $P < 0.01$ versus L929 cells and L929-mock cells treated with hTNF-α for the indicated time. *B,* hTNF-α promoted the interaction of LAPF and p53 ($Ser^{15/18}$) mainly in cytoplasm. L929 cells were treated by hTNF-α (50 ng/mL) for the indicated time, and then the cytoplasmic and nuclear protein fractions were isolated. Immunoprecipitation was performed by anti-LAPF antibody, and the precipitated proteins were detected with anti-p53 ($Ser^{15/18}$) antibody by Western blot analysis. *C,* translocation of phosphorylated p53 ($Ser^{15/18}$) to lysosomes. L929 cells treated with hTNF-α (50 ng/mL), as indicated, were stained with phosphorylated p53 ($Ser^{15/18}$) antibody (*green*). Lysosomes are illustrated as Lyso Tracker Red positive. *D,* accumulation of phosphorylated p53 ($Ser^{15/18}$) and LAPF in lysosomes. Lysosomes were isolated from L929-hLAPF cells and L929-mock cells treated with hTNF-α (10 ng/mL) as indicated. The integrity of the isolated lysosomes was verified by the specific activity of β-hexosaminidase and the presence of LAMP-1 as a marker of lysosomes. Phosphorylated mp53 (Ser^{18}) and LAPF were then detected by Western blot analysis.

However, the reexpression of p53S15A, which is deficient in phosphorylation state of Ser^{15}, could not rescue the decrease in TNF-induced apoptosis in L929-mp53i cells. The data further indicated the vital role of Ser^{15} of p53 in TNF-induced apoptosis.

We further examined how much of other circumstances that are more typically thought of as p53-dependent occurs via LAPF. L929-mLAPFi cells were treated with typical p53-dependent apoptotic stimuli, the DNA damaging drugs, 5-fluorouracil and oxaliplatin, and p53 transfection, and then analyzed for apoptosis by Annexin V/PI staining. The results showed that DNA damaging drugs and p53 transfection–induced cell death was significantly inhibited in L929-mLAPFi cells, compared with that in L929-ctrli and parental

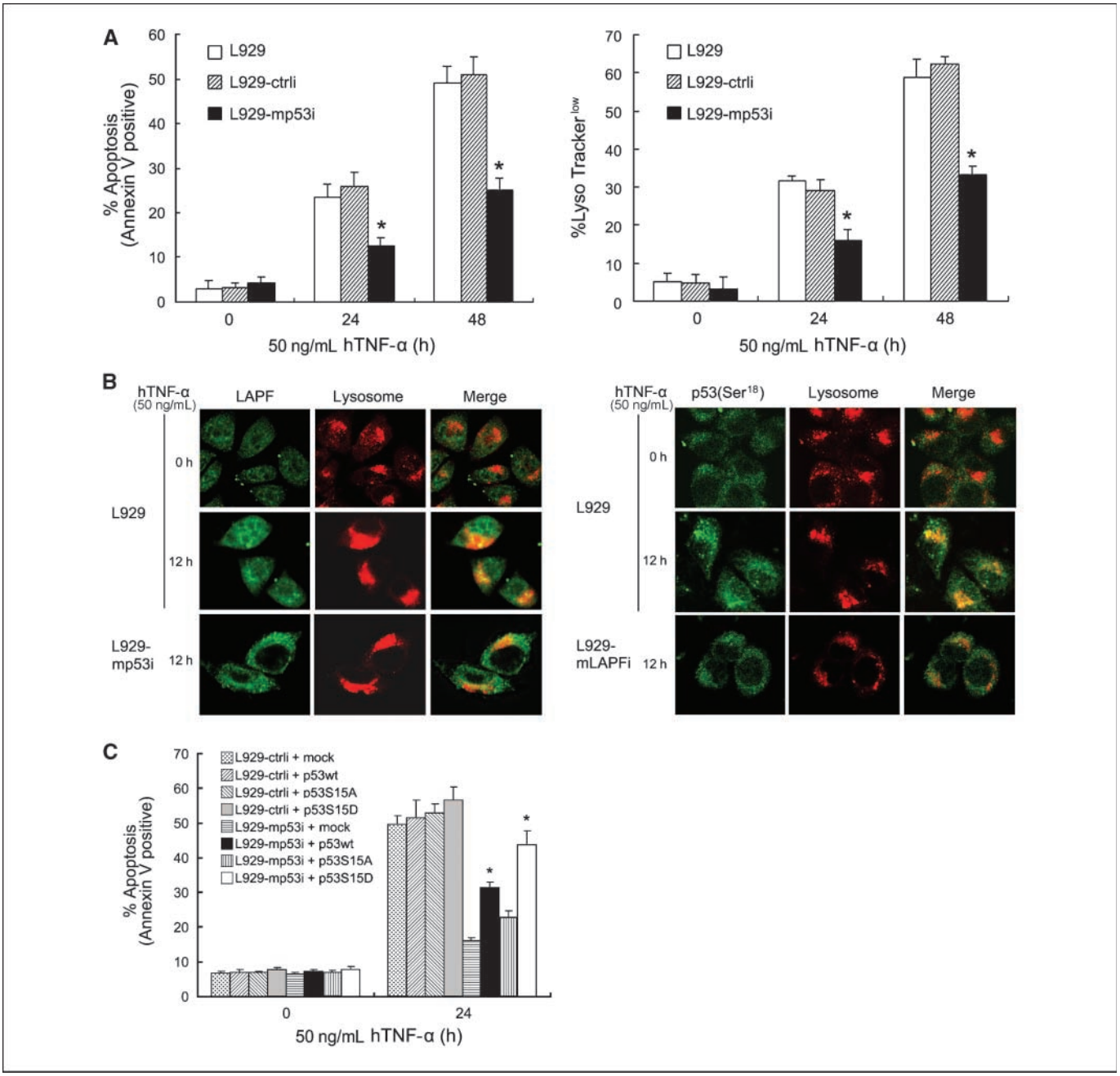

Figure 5. LAPF acts as an adaptor for phosphorylated p53 ($Ser^{15/18}$) to trigger LMP. *A,* silencing of p53 impairs hTNF-α–induced apoptosis and LMP in L929 cells. Cells were treated with 50 ng/mL hTNF-α for the indicated time and stained with Annexin V/PI or Lyso Tracker Red. Apoptosis is represented by the percentage of cells which were Annexin V positive. *Columns,* mean from three independent experiments; *bars,* SD. LMP, *columns,* mean percentage of cells exhibiting reduced fluorescence intensity; *bars,* SD. *, $P < 0.01$ versus L929 or L929-ctrli cells. *B,* translocation of LAPF to lysosomes in L929-mp53i cells and phosphorylated p53 ($Ser^{15/18}$) in L929-mLAPFi cells after hTNF-α stimulation. L929, L929-mp53i cells or mLAPF-silenced L929 cells (L929-mLAPFi) were treated with 50 ng/mL hTNF-α for the indicated time, stained with anti-LAPF antibody or phosphorylated p53 (Ser^{15}) antibody (*green*) and Lyso Tracker Red, and then viewed under a confocal microscope. *C,* p53 could rescue the hTNF-α–induced apoptosis of L929-mp53i cells. Stable L929-mp53i or L929-ctrli cells were transfected with p53wt, p53S15A, p53S15D, or mock vector, respectively. At 24 h after transfection, cells were treated with hTNF-α (50 ng/mL) for 24 h. Cellular apoptosis was detected by Annexin V/PI staining followed by fluorescence-activated cell sorting (FACS) analysis. *Columns,* means of triplicates from one experiment representative of three experiments; *bars,* SD. *, $P < 0.01$ versus L929-mp53i + mock cells.

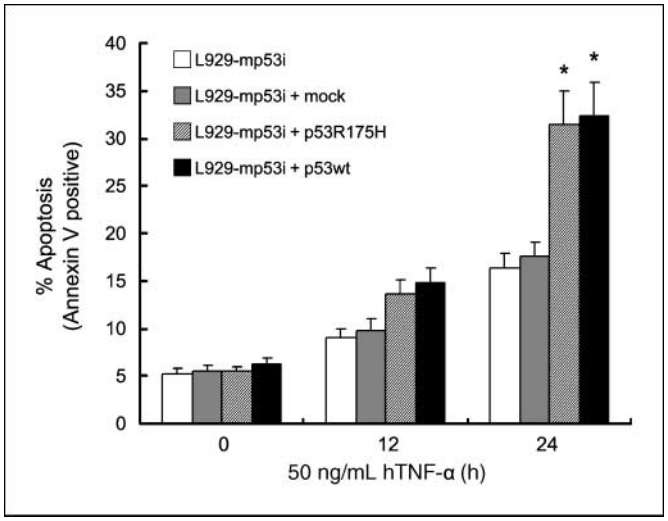

Figure 6. LAPF-initiated apoptosis is transcription independent. Stable L929-mp53i or L929-ctrli cells were transfected with p53wt, p53R175H, or mock vector, respectively. At 24 h after transfection, cells were treated with hTNF-α (50 ng/mL) for the indicated time. Cellular apoptosis was detected by Annexin V/PI staining followed by FACS analysis. *Columns,* means of triplicates from one experiment representative of three experiments; *bars,* SD. *, $P < 0.01$ versus L929-mp53i or L929-mp53i + mock cells.

L929 cells (Supplementary Fig. S3). Therefore, it seems that the p53-dependent cell death might be, at least to a large extent, involved in a LAPF-dependent pathway.

LAPF-initiated and TNF-induced apoptosis is transcription independent. It has been shown that phosphorylated p53 (Ser^{15}) directly targets to lysosomes via interacting with LAPF and results in LMP and apoptosis in LAPF-initiated and TNF-induced apoptosis. To further confirm whether phosphorylated p53 (Ser^{15}) exerted its apoptotic function independent of transcriptional activity, a transcription-deficient mutant, p53R175H, was used in the siRNA rescue assay. The inhibition of hTNF-α–initiated apoptosis in L929-mp53i cells was efficiently rescued by the reexpression of p53R175H, although deficient in transcription activity (Fig. 6). Besides, endogenous expression of $p21^{waf1}$ and Bax, two major p53-regulated genes, remained unchanged during apoptosis (data not shown). These data suggested that LAPF-initiated and TNF-induced apoptosis was independent of p53 transcriptional activity.

Discussion

The present data revealed that there might be another apoptotic pathway through which p53 protein performed a portion of its transcription-independent proapoptosis function. We found that phosphorylated p53 ($Ser^{15/18}$) could target to lysosomes by forming complexes with LAPF and trigger permeabilization of lysosomal membrane, ultimately activating the common apoptotic pathway.

It has been well established that p53 activity is regulated by multiple posttranslational modifications, including phosphorylation and acetylation, under normal physiologic conditions (25). Phosphorylation plays a central role in regulating the stabilization and activity of p53 (26). It had been shown that substitution of all six N-terminal Ser to Ala significantly reduced the ability of p53 to induce apoptosis, and mutations in Ser^{15} and Ser^{20} were primarily responsible for this impairment, indicating the importance of Ser^{15} phosphorylation (27, 28). Phosphorylation of Ser^{15} could reduce the ability of p53 to bind to its negative regulator Mdm2, thus impaired Mdm2-mediated degradation of p53 and resulted in stabilization of p53 (29). Interaction of p53 and Mdm2 had been mapped to the first 19 to 26 residues of p53. Ser^{15} was adjacent to this region, and its phosphorylation affected the p53-Mdm2 interaction (30). On the other hand, Ser^{15} phosphorylation stimulated the binding of p53 with some transcriptional coactivators, such as p300/CBP, TATA box–binding protein, and TATA box–binding protein–associated factors, which were required for transactivation of p53-regulated genes (31–33). In contrast to this opinion, other direct evidence had shown that mutation of Ser^{15} did not affect the ability of p53 to specifically bind to DNA and to transactivate different promoters, indicating the existence of a transcription-independent pathway (27, 34). These conflicting data were most likely due to the different experiment conditions and cell lines used by different authors. In this study, we present a possible transcription-independent pathway that phosphorylated p53 (Ser^{15}) performs its apoptotic activity through directly targeting to lysosomes and resulting in LMP.

In our previous work, we reported that a novel proapoptotic protein LAPF could translocate to lysosomes and initiated LMP, ultimately leading to apoptosis through lysosomal-mitochondrial pathway (17, 27, 34). LAPF was predicted as an adaptor protein because it contained two binding domains, namely, PH and FYVE domain, both lacking catalytic activity. It could thus be postulated that LAPF might recruit potential proteins to lysosomes to trigger LMP. In this study, some evidence supported the functional link between phosphorylated p53 (Ser^{15}) and LMP. First, only lysosome-targeting protein LAPF specifically bound to phosphorylated p53 (Ser^{15}) but not to other phosphorylated forms of p53 (data not shown). The mutation of Ser^{15} could impair the interaction of p53 with LAPF. Secondly, the translocation of phosphorylated p53 (Ser^{15}) to lysosomes preceded LMP in the course of apoptosis. Finally, silencing of endogenous p53 inhibited TNF-α–induced LMP, and silencing of LAPF expression abrogated the lysosomal translocation of phosphorylated p53 (Ser^{15}) concomitant with LMP inhibition. Collectively, these data bring forward a possibility that phosphorylated p53 (Ser^{15}) may be responsible for LMP via accumulating to lysosomes in this apoptotic cell model. Further investigations are needed to confirm the effect of p53 on the permeabilization of lysosomal membrane, such as directly targeting p53 to lysosomes by fusion of p53 with a lysosomal import leader peptide.

Interestingly, a number of observations have shown that p53 can translocate to mitochondria and induce permeabilization of the outer mitochondrial membrane by forming complexes with Bcl-XL and Bcl-2 proteins (9). Directly targeting p53 to mitochondria using import leader fusions was sufficient to trigger mitochondrial membrane permeabilization and apoptosis, confirming the transcription-independent activity of p53 on mitochondria (3). Atractyloside, which could open mitochondrial permeability transition to allow the release of proapoptotic proteins from mitochondria, could induce the release of cathepsins from isolated lysosomes (35). Moreover, Bcl-2 protein, which suppressed cellular apoptosis by regulating mitochondrial permeability transition pores, could effectively prevent the later lysosomal destabilization and, expectably, apoptosis (36, 37). These data strongly suggested that lysosomes shared a similar pore opening mechanism to mitochondria, thereby supporting our speculation that lysosomal membrane stabilization was similarly susceptible to p53.

However, conflicting data was reported by another study, which showed that several chemotherapy drugs could induce LMP independent of p53 activity (38). These drugs elicited significant apoptosis in p53-null HCT116 cells, although they could up-regulate the protein level of p53 in p53 wild-type cells (38). The exact mechanisms of induction of LMP by these compounds remain unknown and are likely to be reversed. Normally, there are multiple apoptotic signal transduction pathways that cooperate to trigger cell death. Organelles, including mitochondria and lysosomes, could sense numerous apoptotic signals and undergo apoptotic alteration. So we speculated that the p53-activated pathway was just one of various mechanisms leading to LMP and might have no cross-talk with the pathway induced by these drugs.

In summary, we reported that phosphorylated p53 (Ser^{15}) could translocate to lysosomes, possibly escorted by a lysosome-localized adaptor protein, LAPF, resulting in permeabilization of lysosomal membranes and transcription-independent apoptosis. These findings provided a new insight into the transcription-independent functions of p53. Further studies are needed to elucidate the exact mechanism of LMP triggered by phosphorylated p53 (Ser^{15}).

Acknowledgments

Received 6/22/2007; revised 8/31/2007; accepted 9/27/2007.

Grant support: National High Biotechnology Development Program of China grant 2006AA02A305, Shanghai Committee of Science and Technology grant 06DJ14011, National Natural Science Foundation of China grants 30121002 and 3050046, and NCET.

The costs of publication of this article were defrayed in part by the payment of page charges. This article must therefore be hereby marked *advertisement* in accordance with 18 U.S.C. Section 1734 solely to indicate this fact.

We thank Prof. Moshe Oren (Weizmann Institute of Science, Israel) for providing the p53 S15A, p53 S15D, and p53 wild-type vectors.

References

1. Wang S, El-Deiry WS. Requirement of p53 targets in chemosensitization of colonic carcinoma to death ligand therapy. Proc Natl Acad Sci U S A 2003;100:15095–100.
2. Roos WP, Kaina B. DNA damage-induced cell death by apoptosis. Trends Mol Med 2006;12:440–50.
3. Marchenko ND, Zaika A, Moll UM. Death signal-induced localization of p53 protein to mitochondria. A potential role in apoptotic signaling. J Biol Chem 2000; 275:16202–12.
4. Caelles C, Helmberg A, Karin M. p53-dependent apoptosis in the absence of transcriptional activation of p53-target genes. Nature 1994;370:220–3.
5. Koumenis C, Alarcon R, Hammond E, et al. Regulation of p53 by hypoxia: dissociation of transcriptional repression and apoptosis from p53-dependent transactivation. Mol Cell Biol 2001;21:1297–310.
6. Haupt Y, Rowan S, Shaulian E, Vousden KH, Oren M. Induction of apoptosis in HeLa cells by trans-activation-deficient p53. Genes Dev 1995;9:2170–83.
7. Kokontis JM, Wagner AJ, O'Leary M, Liao S, Hay N. A transcriptional activation function of p53 is dispensable for and inhibitory of its apoptotic function. Oncogene 2001;20:659–68.
8. Ding HF, Lin YL, McGill G, et al. Essential role for caspase-8 in transcription-independent apoptosis triggered by p53. J Biol Chem 2000;275:38905–11.
9. Mihara M, Erster S, Zaika A, et al. p53 has a direct apoptogenic role at the mitochondria. Mol Cell 2003;11: 577–90.
10. Bennett M, Macdonald K, Chan SW, et al. Cell surface trafficking of Fas: a rapid mechanism of p53-mediated apoptosis. Science 1998;282:290–3.
11. Chen X, Ko LJ, Jayaraman L, Prives C. p53 levels, functional domains, and DNA damage determine the extent of the apoptotic response of tumor cells. Genes Dev 1996;10:2438–51.
12. Yuan XM, Li W, Dalen H, et al. Lysosomal destabilization in p53-induced apoptosis. Proc Natl Acad Sci U S A 2002;99:6286–91.
13. Lotem J, Sachs L. Different mechanisms for suppression of apoptosis by cytokines and calcium mobilizing compounds. Proc Natl Acad Sci U S A 1998;95:4601–6.
14. Vogelstein B, Lane D, Levine AJ. Surfing the p53 network. Nature 2000;408:307–10.
15. Wu GS, Saftig P, Peters C, El-Deiry WS. Potential role for cathepsin D in p53-dependent tumor suppression and chemosensitivity. Oncogene 1998;16:2177–83.
16. Moriwaki Y, Begum NA, Kobayashi M, et al. Mycobacterium bovis Bacillus Calmette-Guerin and its cell wall complex induce a novel lysosomal membrane protein, SIMPLE, that bridges the missing link between lipopolysaccharide and p53-inducible gene, LITAF (PIG7), and estrogen-inducible gene, EET-1. J Biol Chem 2001;276:23065–76.
17. Chen W, Li N, Chen T, et al. The lysosome-associated apoptosis-inducing protein containing the pleckstrin homology (PH) and FYVE domains (LAPF), representative of a novel family of PH and FYVE domain-containing proteins, induces caspase-independent apoptosis via the lysosomal-mitochondrial pathway. J Biol Chem 2005;280: 40985–95.
18. Yang L, Li N, Wang C, et al. Cyclin L2, a novel RNA polymerase II-associated cyclin, is involved in pre-mRNA splicing and induces apoptosis of human hepatocellular carcinoma cells. J Biol Chem 2004;279: 11639–48.
19. Wang X, Li N, Liu B, et al. A novel human phosphatidylethanolamine-binding protein resists tumor necrosis factor α-induced apoptosis by inhibiting mitogen-activated protein kinase pathway activation and phosphatidylethanolamine externalization. J Biol Chem 2004;279:45855–64.
20. Wan T, Zhou X, Chen G, et al. Novel heat shock protein Hsp70L1 activates dendritic cells and acts as a Th1 polarizing adjuvant. Blood 2004;103:1747–54.
21. Roberg K. Relocalization of cathepsin D and cytochrome *c* early in apoptosis revealed by immunoelectron microscopy. Lab Invest 2001;81:149–58.
22. Hoffmann K, Blaudszun J, Brunken C, et al. New application of a subcellular fractionation method to kidney and testis for the determination of conjugated linoleic acid in selected cell organelles of healthy and cancerous human tissues. Anal Bioanal Chem 2005;381: 1138–44.
23. Symons LJ, Jonas AJ. Isolation of highly purified rat liver lysosomal membranes using two Percoll gradients. Anal Biochem 1987;164:382–90.
24. Demoz M, Castino R, Cesaro P, et al. Endosomal-lysosomal proteolysis mediates death signalling by TNF-α, not by etoposide, in L929 fibrosarcoma cells: evidence for an active role of cathepsin D. Biol Chem 2002;383:1237–48.
25. Feng L, Lin T, Uranishi H, Gu W, Xu Y. Functional analysis of the roles of posttranslational modifications at the p53 C terminus in regulating p53 stability and activity. Mol Cell Biol 2005;25:5389–95.
26. Knights CD, Liu Y, Appella E, Kulesz-Martin M. Defective p53 post-translational modification required for wild type p53 inactivation in malignant epithelial cells with mdm2 gene amplification. J Biol Chem 2003; 278:52890–900.
27. Yamauchi M, Suzuki K, Kodama S, Watanabe M. Stabilization of alanine substituted p53 protein at Ser15, Thr18, and Ser20 in response to ionizing radiation. Biochem Biophys Res Commun 2004;323:906–11.
28. Shono T, Tofilon PJ, Schaefer TS, et al. Apoptosis induced by adenovirus-mediated p53 gene transfer in human glioma correlates with site-specific phosphorylation. Cancer Res 2002;62:1069–76.
29. Wang S, Shi X. Mechanisms of Cr(VI)-induced p53 activation: the role of phosphorylation, mdm2 and ERK. Carcinogenesis 2001;22:757–62.
30. Kussie PH, Gorina S, Marechal V, et al. Structure of the MDM2 oncoprotein bound to the p53 tumor suppressor transactivation domain. Science 1996;274: 948–53.
31. Dumaz N, Meek DW. Serine15 phosphorylation stimulates p53 transactivation but does not directly influence interaction with HDM2. EMBO J 1999;18: 7002–10.
32. Farmer G, Colgan J, Nakatani Y, Manley JL, Prives C. Functional interaction between p53, the TATA-binding protein (TBP), andTBP-associated factors *in vivo*. Mol Cell Biol 1996;16:4295–304.
33. Grossman SR. p300/CBP/p53 interaction and regulation of the p53 response. Eur J Biochem 2001;268: 2773–8.
34. Ashcroft M, Kubbutat MH, Vousden KH. Regulation of p53 function and stability by phosphorylation. Mol Cell Biol 1999;19:1751–8.
35. Vancompernolle K, Van HF, Pynaert G, et al. Atractyloside-induced release of cathepsin B, a protease with caspase-processing activity. FEBS Lett 1998;438: 150–8.
36. Zhao M, Eaton JW, Brunk UT. Protection against oxidant-mediated lysosomal rupture: a new anti-apoptotic activity of Bcl-2? FEBS Lett 2000;485:104–8.
37. Zhao M, Eaton JW, Brunk UT. Bcl-2 phosphorylation is required for inhibition of oxidative stress-induced lysosomal leak and ensuing apoptosis. FEBS Lett 2001; 509:405–12.
38. Erdal H, Berndtsson M, Castro J, et al. Induction of lysosomal membrane permeabilization by compounds that activate p53-independent apoptosis. Proc Natl Acad Sci U S A 2005;102:192–7.